ELSEVIER

Journal of Chromatography A, 928 (2001) 1–12

JOURNAL OF CHROMATOGRAPHY A

www.elsevier.com/locate/chroma

Evaluation of frontal chromatograms

U. Wenzel*

Forschungszentrum Jülich GmbH, Institut für Sicherheitsforschung und Reaktortechnologie, P.O. Box 1913, D-52425 Jülich, Germany

Received 13 February 2001; received in revised form 9 July 2001; accepted 11 July 2001

Abstract

Frontal chromatograms were investigated at low effluent concentrations, and deviations from the pertinent theory of chromatography were found in that region. These deviations are explained by a prerun in the column occurring between column wall and adjacent vertical particle layer. A model was devised for adapting these deviations to a mathematical function. According to that model, frontal chromatograms have an additional inflection point at low effluent concentrations with coordinates defined by the geometry of the column and the particles of the column bed. These coordinates are only altered by a packing density leading to particle distortion; on the premises of a reproducible column packing, these values are neither affected by kinetic parameters nor by a deterioration of the active particle surface. The experimental verification shows that the model can be employed to describe frontal chromatograms up to the second inflection point, when the effluent concentration reaches half of the feed concentration. A technical application is indicated in the paper.

Keywords: Frontal chromatograms; Wall effect model

1. Introduction

Frontal chromatography is a term that has been defined by Tiselius [1] and refers to a mode of operating a chromatographic column. A feed solution is permanently conveyed through the column, the solutes interacting with the column bed are retained until the bed is saturated and the solutes appear in the column effluent. Then, column loading is terminated, the column is washed to remove feed solution from the interstitial column volume and the retained solutes are subsequently stripped. In contrast to elution chromatography, frontal chromatography cannot be used to isolate solutes from each other, but it is an ideal method for partitioning a solution into fractions of solutes with similar properties (e.g., poisonous from non-poisonous compounds, ionogenic from non-ionogenic species, radioactive nuclides from inactive matter, α-emitters from fission products). Within these limits, this method can serve two purposes:

– Either to recover a solute from the feed; in this case, the column is operated up to saturation. The retained solute constitutes the process product and small losses in the column effluent are acceptable. Such processes are only feasible when the solute is selectively retained by the column bed.

– Or to decontaminate a solution from solutes; then the separation is terminated long before column

*Tel.: +49-2461-615-789; fax: +49-2461-612-450.

0021-9673/01/$ – see front matter
PII: S0021-9673(01)01114-1

saturation when the very first breakthrough of the least retained solute is observed in the effluent. The process product is the decontaminated column effluent and the retained solutes are considered as waste.

In organic chemistry, frontal chromatographic processes are suggested as a final purification step for the preparation of some rare compounds. The pertinent references deal, however, more with the theoretical aspects of preparative frontal chromatography than with technical applications [2–4]. The best known example of a decontamination is the desalination of water by ion exchange, actually the only frontal chromatographic procedure that has found a broad technical application [5].

In our field of research, the nuclear fuel cycle, attempts have been made to introduce frontal chromatographic processes in the reprocessing tail-end and radioactive waste management. In several reprocessing plants, the Pu product streams have been purified with anion-exchange resins [6]. Pu is sorbed on the resin as a hexa–nitrato complex, while the impurities are washed from the column with concentrated and diluted nitric acid. Cation-exchange resins are also used for Pu purification. Pu is reduced to Pu(III) and loaded onto the column in a mixture of diluted nitric and sulfuric acid. The impurities, mainly UO_2^{2+}, are washed from the column with 0.025 *M* $(NH_3OH)_2SO_4$ and Pu is recovered with strong nitric acid. A compilation of such processes is given in Ref. [7]. Frontal chromatography is also employed for recovering Am from molten salt extraction wastes [8]. In a first frontal chromatographic step, Pu is removed from the feed solution by anion exchange in 7 *M* HNO_3, then Am is recovered from the first column effluent on an Amberlite XAD 4 resin impregnated with CMP (dihexyl-*N*,*N*-diethylcarbamoylmethyl phosphonate). The first step is an example of a decontamination, the second of a purification process.

Most of the above mentioned Pu recovery processes are operated in a dual purpose manner. Apart from purifying Pu, they shall also serve to decontaminate the column effluent from Pu. From that point of view, however, the processes show a rather poor performance. In Am production [8], the Am product was contaminated with about 0.1% Pu; in Pu recovery [7], the column effluent contained about 0.5% (~0.01 g Pu/l) of the Pu feed. In most countries, such liquids would still be considered as Pu-bearing fissile waste, e.g., in Ref. [9]. This performance reveals the general weakness of a frontal chromatographic decontamination process. Operated in a non-equilibrated state, the process control depends on real-time monitoring of the column effluent; thus, the detection limits of the monitor mainly determine the quality of the product and not the column layout, the chemical system or the separation kinetics chosen. In nuclear chemistry, appropriate detectors show rather high background rates especially for α- and β-emission, which badly impair the detection limits and, thus, the decontamination factors achieved.

As we were attracted by the general versatility of frontal chromatography for partitioning and decontaminating aqueous solutions, we evaluated frontal chromatograms in order to find regularities in the low effluent concentration region that may help to overcome the deficiencies encountered in real-time monitoring. Empirically, we found that the deviations from the theoretical chromatograms indicate a prerun [10] which is likely due to the finite nature of the chromatographic column. We have now designed a model to describe this effect mathematically and have verified the model experimentally. The results of our investigation are set forth in this paper.

2. Experimental

This study was performed within the framework of our R&D program on partitioning high level radioactive waste solutions. Therefore, we devised our experiments such that our solid-phase extraction systems were capable of retaining selected fission products and actinide nuclides, and we set up our detection systems accordingly.

2.1. Chemicals and equipment

If not otherwise stated, chemicals and reagents were purchased from Merck (Darmstadt, Germany)

or Riedel-de Haën (Hanover, Germany) in analytical-reagent grade quality. CMPO (*n*-octyl phenyl carbamoyl-*N*,*N*-diisobutyl-methyl phosphine oxide) was obtained from Elf Atochem Deutschland (Düsseldorf, Germany). The resins Amberchrom CG 71 (polymethacrylate) and Amberlite XAD 7 (polyacrylester) were procured from Sigma–Aldrich, (Dept. Supelco, Deisenhofen, Germany). The actinide nuclides and radioactive fission product isotopes were supplied by Isotopen Dienst (Waldburg, Germany). α-Spectra, as provided by the supplier, showed no impurities in the nuclide solutions within the detection limits; the β-emitters decay to stable nuclides that do not interfere with the detection.

For our separation unit, we used columns made out of Perspex and machined in the laboratory workshop. Fittings, valves and tubes were supplied by BEST (Bornheim, Germany) the local representative of Swagelok, USA. We used membrane pumps from Leva (Leonberg, Germany). All other pieces of equipment consisted of ordinary labware.

Process control was carried out with the radioactivity monitor LB 508 C, from EG&G Berthold (Bad Wildbach, Germany), now merged with Perkin-Elmer, which we equipped with the custom-made detector flow cell WUW-ML 10 [11]. We dismantled the monitor and installed the detection unit (detector cell and chamber, multipliers and preamplifiers) together with the separation unit inside a hood, while the electronic parts together with the processor from Sontag (Waldfeucht, Germany) were left outside the hood. For comparison purposes, we also performed off-line process control and calibration analyses of the radioisotopes with the liquid scintillation counter Tricarb 1900CA from Canberra Packard (Dreieich, Germany) using the scintillator Instant Scint Gel plus from the same company.

2.2. Resin preparation and column packing

Various amounts of CMPO (5 g≤m CMPO≤37.5 g) are dissolved in ~100 ml TBP (tri-*n*-butyl phosphate) with gentle heating. The solution is cooled down to room temperature and then made up with TBP to 150 ml. Approximately 250 ml C_6H_{12} (cyclohexane) is added and 100 g Amberchrom CG 71 (particle diameter 70–100 μm) suspended in the diluted solution. C_6H_{12} is then evaporated at room temperature, and the last traces of this solvent are removed at 60°C. The yield of the dry, coated resin amounts to 244 g with an average particle diameter of 112 μm.

Subsequently, the dry resin is sieved and fractions with sizes of 70–100, 100–125 and 125–160 μm were collected. Resin beads of the same fraction are suspended in water and the suspension is filled into a pressurized vessel. Using a circulatory system (vessel – column – pump – vessel), the suspension is conveyed into the column, which is closed at the lower end with a frit. During packing, the pressure drop in the system is kept constant by varying the flow. When the column is completely packed, the flow is discontinued and the upper column end covered with another frit, so that the column can be operated in either direction. The quality of the column packing is controlled by determining the porosity (interstitial column volume/column volume) which routinely amounts to 0.45.

2.3. Operation of the separation unit

The separation unit serves to carry out the two process stages of loading and elution. It consists of the supply (feed and strip) and removal (eluate and product) tanks, the pump, the column and the process monitoring devices, i.e., the on-line detector and the sampling stations for off-line analyses (Fig. 1). We used simple overflow vessels for the sampling stations and placed one station in each loop in order to avoid cross contamination. We determined the void volume of the stages between the upper three port valve and detector (on-line mode) or sampling station (off-line mode) using a Cs-137 feed and measured the flow by time control and conveyed volume in the removal tanks. Usually, we determined the solute concentration in the feed by acquiring complete chromatograms during loading. It was thus possible to avoid separate detector calibration. However, we could also bypass the column to measure the feed solution and clean the detector prior to the operating the column.

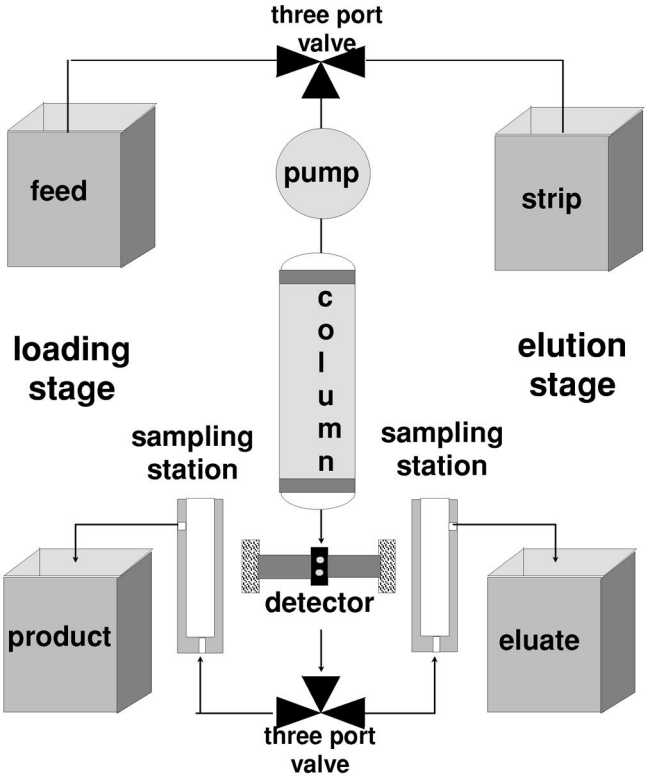

Fig. 1. Simplified drawing scheme of the separation unit.

3. Results and discussion

We started our investigations by confirming the results as obtained in Ref. [10], and on this basis, we designed a model in order to mathematically assess the deviations noted. Finally, we verified the model experimentally. Relevant figures and values presented in this paper are corrected for background and void volume. With respect to the extraction system, we confined our considerations strictly to the linear part of the relevant extraction isotherms, as the solute concentrations in our envisaged application, the actinide partitioning of high and medium level radioactive waste solutions, lie in the order of 10^{-4} mol/l.

3.1. Preliminary results

Frontal chromatograms are usually displayed as the volume-dependent ratio of effluent and feed concentration. We have depicted such a chromatogram in Fig. 2, using Cm-244 as the solute. According to Glueckauf [12], frontal chromatograms can be mathematically described by the cumulative, standardized normal distribution function:

$$c_{\text{effluent}}/c_{\text{feed}} = (2\pi)^{-0.5}\int_{-\infty}^{t} e^{-t^2/2}\mathrm{d}t = \mathrm{erf}(t) \qquad (1)$$

where erf(t) is a tabulated function [13]. When applied to chromatograms, the argument t is composed of:

$$t^2 = N\frac{(V_{\text{BT}} - V)^2}{V_{\text{BT}}V} \qquad (2)$$

where N = number of theoretical plates, V = effluent volume, and V_{BT} = effluent volume of the curve's

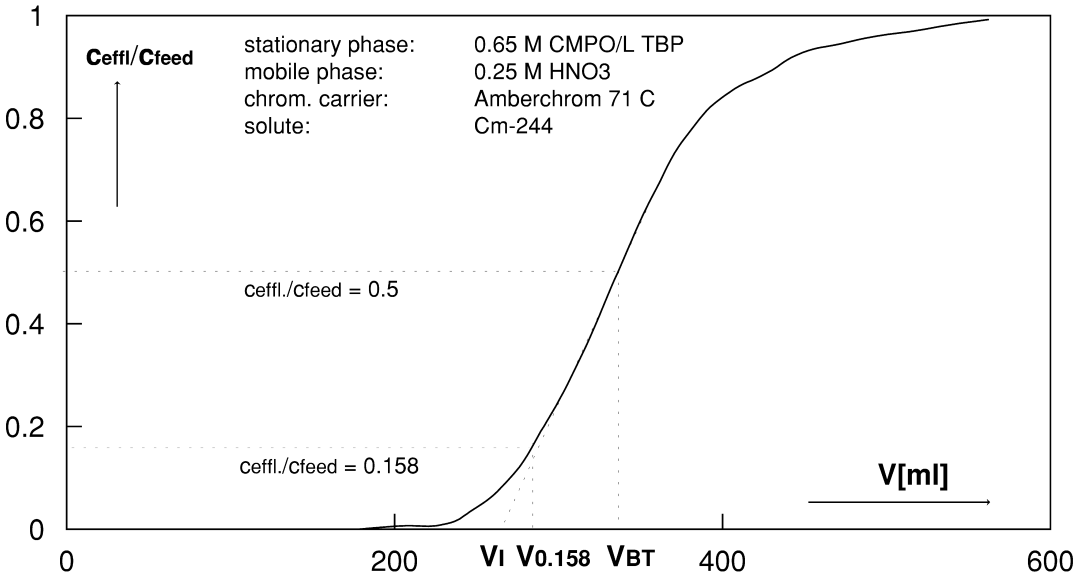

Fig. 2. Frontal chromatogram of a single solute.

inflection point at $c_{\text{effluent}}/c_{\text{feed}} = 0.5$ (breakthrough volume).

The breakthrough volume V_{BT} is independent of kinetic parameters, it is a measure of the capacity of the chromatographic support according to the equation:

$$V_{\text{BT}} = K_{\text{cs}} V_{\text{cs}} \tag{3}$$

where K_{cs} = distribution coefficient applied to the chromatographic support and V_{cs} = volume of the chromatographic support.

For an acquired frontal chromatogram, the breakthrough volume V_{BT} is established graphically at the corresponding concentration ratio of 0.5 (see Fig. 2), while N is calculated using Eq. (2) at a fixed effluent concentration ratio ($c_{\text{T}}/c_{\text{feed}}$), the tabulated t value T and the corresponding effluent volume V_{T}. Usually, a ratio of 0.158 is chosen, as $(T_{0.158})^2$ equals 1 and N fits the equation:

$$N = \frac{V_{\text{BT}} V_{\text{T}\,0.158}}{(V_{\text{BT}} - V_{\text{T}\,0.158})^2} \tag{4}$$

We evaluated the chromatogram in Fig. 2 accordingly and found a rather large uncertainty in determining $V_{\text{T}\,0.158}$, as it lies in the non-linear part of the curve. Thus, we decided to base our evaluation on V_{BT} and the first derivative of Eq. (1). This procedure leads to the following equation for N:

$$N = \frac{\pi}{2} \cdot \frac{V_{\text{BT}}^2}{(V_{\text{BT}} - V_{\text{I}})^2} \tag{5}$$

where V_{I} = intercept of the tangent at V_{BT} with the V-axis.

V_{I} can be determined either by linear regression or graphically. The N values as derived from Eqs. (4) and (5) should be the same. However, we found an N value of 31 using Eq. (4) (hereinafter referred to as N_{T}) and an N value of 42 using Eq. (5) (hereinafter referred to as N_{BT}) for the chromatogram in Fig. 2. We could confirm the difference between N_{T} and N_{BT}, when we compared chromatograms acquired with the same chromatographic system but with different linear flow velocities u. Such a comparison is done using the height equivalent of a theoretical plate H [14]:

$$H = L_{\text{C}}/N = A + B/u + Cu \tag{6}$$

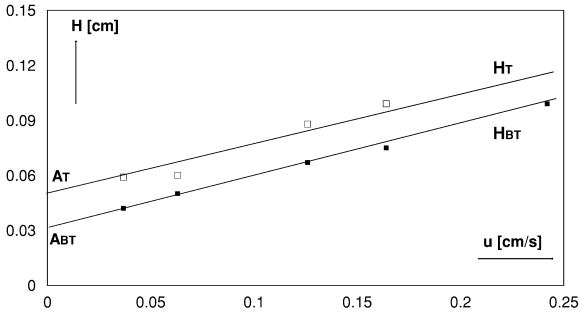

Fig. 3. Height equivalent of a theoretical plate as function of the linear flow velocity.

where L_C = column length, A = term considering the eddy diffusion, B = term considering the longitudinal diffusion and C = term considering the sorption kinetics.

Under routine operational conditions, the term B/u can be ignored and $H(u)$ becomes a linear function with a slope C and A as the intercept of the H-axis. We obtained different straight lines (Fig. 3) with the $H_T(u)$ $(=L/N_T)$ as well as the $H_{BT}(u)$ $(=L/N_{BT})$ values. As expected, the H_T values were much more scattered around the line, the A_T value was higher than the A_{BT} value, but both lines showed the same slope.

Subsequently, we took T values from a number of c/V pairs collected from our chromatograms. We calculated the corresponding the N_T-values using Eq. (2). Fig. 4 shows the N_T values as a function of the effluent volume at various flow velocities. The N_T values are almost constant at low effluent volumes and are independent of the flow velocity in that region. They increase, however, differently at higher effluent volumes up to a maximum value, when the breakthrough volume is attained ($V=V_{BT}$). In general, lower N values at low effluent volumes indicate an early breakthrough of the solute in the column effluent. We interpreted that behavior as a prerun of a small feed portion, which would effect a higher concentration rise at low effluent volumes than theoretically expected, but become negligible around and above the inflection point.

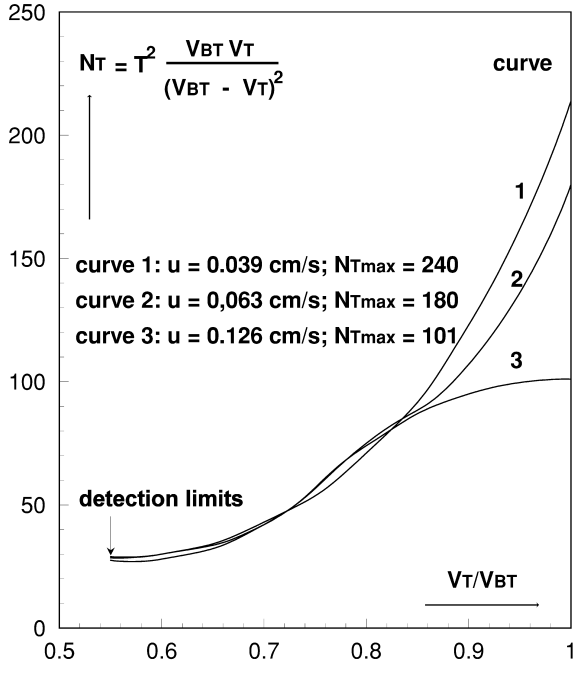

Fig. 4. Dependence of the theoretical plate number from effluent volume and concentration.

3.2. Wall effect model

We ascribe the assumed prerun to the finite nature of the column. The channels between column wall and the adjacent vertical particle layer are surrounded by less extractant than the channels in the column interior, since only the particles carry the extractant or the active groups (ion-exchange, adsorption chromatography). Thus, an early breakthrough of the solutes should occur at the end of these wall channels.

This effect of the column wall must not be confused with those wall effects as postulated first by Knox et al. [15] and eventually confirmed by Farkas et al. [16]. According to these authors, a region with a thickness of ~30 particle diameters at the column wall has a higher density and a lower porosity than the core of the column bed. The authors investigated the effect of the denser packing on elution chromatograms and found a slight shifting of the peak maximum and a strong tailing of the peak. Applied to frontal chromatograms, the denser packing would yield a shifting of the inflection point to larger

effluent volumes and, beyond this point, a flattening of the curve at higher concentrations. We have observed such effects, but deemed them insignificant for frontal chromatographic decontamination processes, which operate in the low effluent concentration region. Thus, we disregarded these wall effects in our study.

Another wall effect has been visualized by Shalliker et al. [17] using samples of J_2 dissolved in CCl_4 on C_{18} silica spheres. Without being retained by the stationary phase, J_2 moves much faster at the wall through the column. This is due to the higher linear velocity of the mobile phase at the column wall. According to experimental data [18] and their mathematical evaluation [19], the velocity in those channels adjacent to the column wall is about 20% higher than the average linear velocity in the column. We are well aware that this wall effect should affect our assumed prerun, however we did not include this effect in our further considerations.

We designed a model (Fig. 5) in order to quantify the supposed prerun, and we established the following presuppositions:

(1) The sorption in column wall and interior channels should follow the same regularities.

(2) We assume a simple cubic structure in accordance with the measured porosity.

(3) We disregard any particle distortion by the operational pressure.

(4) We ignore interactions between wall and interior channels.

Following these assumptions, prerun and main stream have individual breakthrough curves, which pile up on each other, and Eq. (1) can be transformed into:

$$c_{\text{effluent}}/c_{\text{feed}} = a\ \text{erf}(w) + b\ \text{erf}(i) \tag{7}$$

Let the arguments w and i be composed following Eq. (2):

$$w^2 = N \cdot \frac{(V_{\text{BT w}} - V)^2}{V_{\text{BT w}} V} \quad i^2 = N \cdot \frac{(V_{\text{BT i}} - V)^2}{V_{\text{BT i}} V} \tag{8}$$

For defining constants a and b, we used the flow fraction model (Fig. 5, left part). The column wall is inert against the mass transfer. Thus, less active matter is available in the wall channels. Assuming a sufficiently high theoretical plate number N and $w \rightarrow \infty$, the concentration in the wall channels would

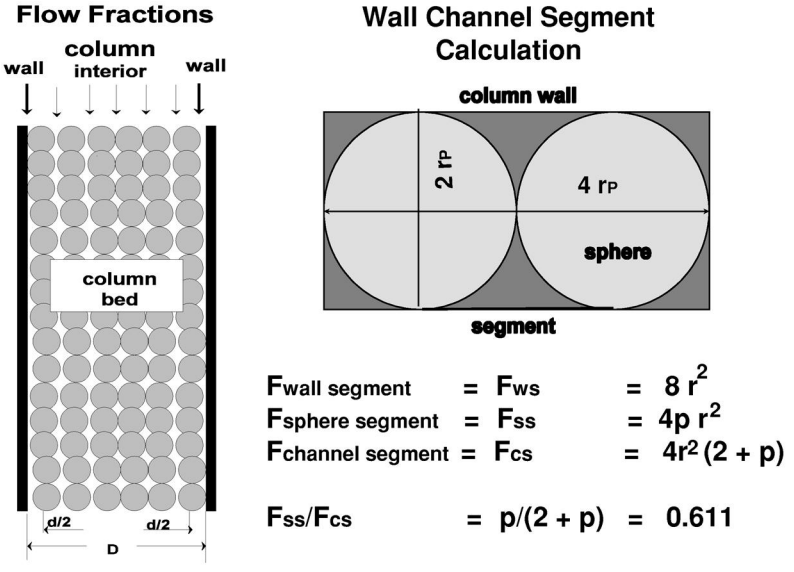

Fig. 5. Wall effect model, left: flow fractions, right: wall channel segment calculation.

reach c_{feed}, while decontaminated mobile phase would still flow through the interior channels and dilute the solute of the wall channels in the column outlet. According to the model, the dilution can be expressed by the volume ratio of wall and total column channels (interstitial column volume V_{icv}). V_{icv} amounts to:

$$V_{icv} = 1/4\pi\phi_C^2 L_C E \tag{9}$$

In accordance with our model, the wall channel diameter corresponds to the particle radius, and the wall channel volume V_w fits the equation:

$$V_w = 1/4\ \pi \cdot [\phi_C^2 - (\phi_C - \phi_P)^2] \cdot L_C E \tag{10}$$

The ratio V_w/V_{icv}yields:

$$\frac{1/4\pi L_C E \cdot [\phi_C^2 - (\phi_C - \phi_P)^2]}{1/4 L_C E \pi \phi_C^2} \approx 2\phi_P/\phi_C \tag{11}$$

where ϕ_P = particle diameter, L_C = column length, ϕ_C = column diameter and E = porosity and, thus:

$$a\ \mathrm{erf}(w \to \infty) = a \approx 2\phi_P/\phi_C \tag{12}$$

At a 100% breakthrough, Eq. (7) would read:

$$\begin{aligned} c_{effluent}/c_{feed} &= a\ \mathrm{erf}(w \to \infty) + b\ \mathrm{erf}(i \to \infty) \\ &= a + b = 2\phi_P/\phi_C + (1 - 2\phi_P/\phi_C) \\ &= 1 \end{aligned} \tag{13}$$

We assessed the individual breakthrough volumes $V_{BT\ w}$ and $V_{BT\ i}$ in Eq. (8), using the right part of Fig. 5. We considered a wall channel segment formed by two spheres and the opposite column wall. We compared the active surface of the segment (F_{SS}) with the total segment surface (F_{CS}) at the wall:

$$F_{CS} = F_{SS} + F_{WS} \tag{14}$$

The active surface is formed by 1/2 of two spheres ($=4\pi r_P^2$), the wall surface amounts to $8r_P^2$ (r_P = particle radius). We obtain a ratio of:

$$\begin{aligned} F_{SS}/F_{CS} &= 4\pi r_P^2/4r_P^2 \cdot (2 + \pi) = \pi/(2 + \pi) \\ &= 0.611 \end{aligned} \tag{15}$$

The interior channels are completely surrounded by active surfaces, and the above ratio equals 1. We now compare the volumes of the chromatographic support at the wall and in the column interior:

$$\begin{aligned} (L_C F_{SS}/F_{CS})_w/(L_C F_{SS}/F_{CS})_i &= V_{CS\ w}/V_{CS\ i} \\ &= \{\pi/(2 + \pi)\}/1 = 0.611 \end{aligned} \tag{16}$$

Applying Eq. (3) to the partial chromatographic support volumes, we conclude for the individual breakthrough volumes that $V_{BT\ w} = 0.611 V_{BT\ i}$. $V_{BT\ i}$ corresponds to an effluent concentration ratio of:

$$\begin{aligned} c_{BT\ i} &= 1/2 \cdot (1 - 2\phi_P\phi_C) + 2\phi_P\phi_C \\ &= 0.5 + \phi_P\phi_C \end{aligned} \tag{17}$$

which is still on the linear part of the chromatogram. Using Eq. (5), we calculate $V_{BT\ i}$ as follows:

$$\frac{V_{BT\ i} - V_{BT}}{\phi_P/\phi_C} = \frac{V_{BT} - V_I}{0.5} = 2(\pi/2N)^{0.5} V_{BT} \tag{18}$$

resulting in a $V_{BT\ i}$ value of:

$$V_{BT\ i} = V_{BT} \cdot \{1 + 2\phi_P/\phi_C \cdot (\pi/2N)^{0.5}\} \tag{19}$$

Under routine conditions in chromatography, $\phi_P/\phi_C \leq 0.01$ and $N \geq 10$, yielding a $V_{BT\ i}$ value that differs less than 1% from V_{BT} allowing the approximation:

$$V_{BT\ i} \approx V_{BT} \tag{20}$$

Summarizing the above derivations, we rewrite Eq. (7):

$$\begin{aligned} c_{effluent}/c_{feed} &= 2\phi_P/\phi_C\ \mathrm{erf}\left\{ \sqrt{N} \cdot \frac{V - 0.611 V_{BT}}{(0.611 V_{BT} V)^{0.5}} \right\} \\ &+ (1 - 2\phi_P/\phi_C)\ \mathrm{erf}\left\{ \sqrt{N} \cdot \frac{V - V_{BT}}{(V_{BT} V)^{0.5}} \right\} \end{aligned} \tag{21}$$

This function describes a frontal chromatogram within the region $0 \leq V \leq V_{BT}$. Above V_{BT}, we would notice deviations caused by those wall effects as described in Refs. [15] and [16].

3.3. Experimental verification of the model

As stated before, we chose chromatographic systems capable of partitioning high level radioactive waste solutions. We used Amberchrom 71 C resins coated with a CMPO/TBP solution as the stationary phase and actinide and lanthanide radioisotopes as solutes. We first attempted to obtain a chromatogram that showed the two predicted inflection points. We divided the column effluent into very small fractions and determined the solute concentration in the individual fractions by off-line liquid scintillation counting. Due to the large difference between the concentration ratios, we needed two scales for the same chromatogram to prove the existence of the two inflection points in Fig. 6, a logarithmic scale to show the $V_{BT\ w}$ inflection point and a linear scale to show the V_{BT} inflection point. We obtained a $V_{BT\ w}$ value of 100 ml and a V_{BT} value of 167 ml, each one corrected for the void volume V_v. The ratio of the

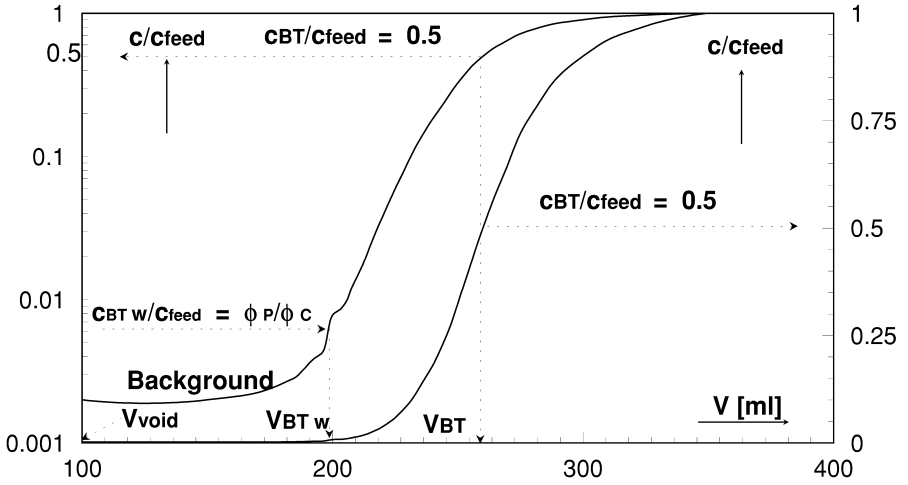

Fig. 6. Front chromatogram with two branches; left curve: logarithmic, right curve: linear concentration ratio scale.

Table 1
Determination of the ratio $V_{BT\ w}/V_{BT}$

Nuclide	Medium	V_{BT} (ml)	u (cm/s)	N	$V_{BT\ w}/V_{BT}$
Cm-244(III)	1.0 *M* HNO_3	258	0.133	**15**	**0.55**
Cm-244(III)	1.0 *M* HNO_3	258	0.063	62	0.64
	1.5 *M* HNO_3	308	0.034	89	0.62
Cm-244(III)	2.1 *M* HNO_3	152	0.039	207	0.63
	0.001 *M* Ce^{3+}	154	0.063	180	0.63
		153	0.126	134	0.64
Cm-244(III)	2.0 *M* HNO_3	58	0.079	74	0.63
	0.005 *M* Ce^{3+}				
Eu-152(III)	2.0 *M* HNO_3	60	0.033	47	0.60
	0.005 *M* Ce^{3+}				
U-233(VI)	2.0 *M* HNO_3	80	0.014	39	0.62
Pu-238(IV)	0.5 *M* H_3PO_4	191	0.022	**11**	**0.53**
	0.1 *M* Ce^{3+}				

two volumes amounted to 0.6, i.e., very close to the calculated value of $\pi/(\pi+2)$. The concentration ratio corresponding to $V_{BT\,w}$ was determined as 0.0068. The column diameter was 2 cm, and we used the particle fraction with an average diameter of ~140 μm. Thus the ratio ϕ_P/ϕ_C of 0.007 lies within the measurement uncertainty (±10%).

We then varied the mobile phase, the linear velocity and the solutes by always using the same column with a length $L=10$ cm, $\phi_C=1.4$ cm and 7.9 g chromatographic support with $\phi_P=0.011$ cm coated with 4.9 ml of a 0.32 *M* CMPO/L TBP solution. Again, we fractionated the column effluent, measured the solute concentration in the individual fractions and determined the volume corresponding to the concentration ratio of 0.008 ($=\phi_P/\phi_C$). The results are summarized in Table 1. With the exception of two values displayed in Table 1 in bold type, this concentration ratio corresponded to an average volume ratio of ~0.62, well within the measurement uncertainty of the predicted value.

Finally, we investigated the effect of the geometrical parameters. As we had only three resin fractions available, we varied the column diameters as well. Again, we applied effluent fractionation and off-line scintillation counting for the concentration measurement. We were confronted with a rather high background due to contamination of the chromatographic unit and obtained results with a high uncertainty. Nevertheless, the measured values fit the expected equation (Fig. 7):

$$c_{BT\,w}/c_{feed} = \phi_P/\phi_C \tag{22}$$

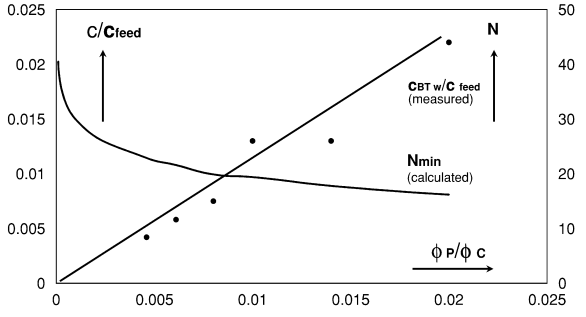

Fig. 7. Concentration ratio at the wall fraction inflection point and minimum number of theoretical plates as function of the particle/column geometry.

3.4. Deviations from the model

We noted two outliers in Table 1, each one accompanied with a very low value for the number of theoretical plates *N*. We ascribe these outliers to an overlapping of wall and interior fraction. Such an interference must be noticeable if $c_{i\,BT\,w}$, the concentration of the effluent's interior fraction at the first inflection point ($V=V_{BT\,w}=0.611V_{BT}$), exceeds the measurement uncertainty σ of $c_{BT\,w}$. Assuming a $\sigma_{c\,BT\,w}$ value of ±25%, we could establish the condition for a distinct wall fraction breakthrough point:

$$(1-2\phi_P/\phi_C)\,\mathrm{erf}(i_{BT\,w}) \le 0.25\phi_P/\phi_C \tag{23}$$

and, thus, define a minimum number of theoretical plates N_{min} which would be necessary for obtaining a distinct breakthrough point of the wall fraction:

$$N_{min} \ge (i_{BT\,w})^2 \cdot \frac{(0.611V_{BT})^2}{(V_{BT}-0.611V_{BT})^2}$$

$$= 2.47\,(i_{BT\,w})^2 \tag{24}$$

Eqs. (17) and (18) demonstrate that N_{min} depends on the chosen particle/column geometry; $\mathrm{erf}(i_{BT\,w})$ can be calculated using Eq. (17); the corresponding value for $i_{BT\,w}$ is tabulated [13]. The number of theoretical plates for the outliers (see Table 1) is much lower than the required N_{min} (≈20, see Fig. 7), which provides evidence for our assumption of an overlapping.

Other deviations that may occur are associated with the presuppositions for establishing the wall effect model. We assumed a simple cubic structure following our results on the porosity determination ($E=0.45$). However, larger inhomogeneities especially at the column wall would increase the concentration and decrease the volume ratio of the wall fraction breakthrough point.

The reversed effect would be obtained by a particle distortion. The particles would be squeezed against the column wall, the channel diameter would be reduced and the effective channel surface ratio enhanced. The wall fraction breakthrough point

would appear at a lower concentration and a higher volume ratio. Such denser column packing occurs routinely during the preparation of high-performance liquid chromatography (HPLC) columns [20] at high pressure. We observed such an effect when using Amberlite XAD 7, a polyacryl ester, as chromatographic carrier. During column packing and operation, we had a much higher pressure build-up, and we needed more resin than expected to fill the column. With a $\phi_P/\phi_C = 0.017$, the concentration ratio at the wall fraction breakthrough point amounted to 0.01 and the corresponding volume ratio to 0.65.

With respect to the other two assumptions, we could neither confirm nor confute them in our experiments; they are simply best estimates. We could not determine $N_{BT\ w}$, but only assess that this value was in the same order of magnitude as N_{BT}. Due to the higher linear velocity of the mobile phase at the column wall, $N_{BT\ w}$ should be lower than N_{BT}. However, $N_{BT\ w} \neq N_{BT}$ would not change the two breakthrough points of the front chromatogram. With respect to interactions between wall and interior channels, we could not notice any effect under the prevailing experimental conditions, so that we feel justified in ignoring them.

4. Conclusions

Within the framework of nuclear waste partitioning, we investigated frontal chromatograms and found deviations from the theoretical function at low effluent concentrations. We ascribed this effect to a prerun occurring between column wall and adjacent vertical particle layer. We designed a model that allows us to adapt these deviations to a mathematical function, assuming that prerun and main stream follow the cumulative standardized normal distribution function.

We verified our model experimentally. Within its defined region, this function should have two inflection points, one for the prerun and one for the main stream. We could show these inflection points experimentally by choosing rather unusual ratios of column and particle diameter ($50 \leq \phi_C/\phi_P \leq 200$). The inflection points do not depend on operational kinetic parameters, but only on the active surface available for the individual streams and the particle/column geometry. When the column is frequently reused, the resin bed may deteriorate and the location of the individual breakthrough points may be altered, but their volume and concentration ratio will remain constant.

Consequently, it is possible to determine the location of the prerun's breakthrough point, even if its effluent concentration lies below the detection limits of available on-line monitors. As an entire front chromatogram must be acquired for that purpose, a technical application may not be obvious and certainly not feasible using a one column separation set. However, a unit consisting of the array column – detector – column can be devised, which is then operated up to the measurable main stream breakthrough point of the first column, while the effluent of the second column is practically free of solute contamination. We intend to describe the operation of such a column unit in our next paper.

References

[1] A. Tiselius, Akad. Kemi Mineral. Geol. 16a (1943) 1.
[2] P. Dantigny, Y. Wang, J. Hubble, J. Howell, J. Chromatogr. 545 (1991) 27.
[3] D. Hill, P. Mace, D. Moore, J. Chromatogr. 523 (1990) 11.
[4] G. Guiochon, A. Katti, Chromatographia 24 (1987) 165.
[5] J. Weiss, Handbuch der Ionenchromatographie, Verlag Chemie, Weinheim, 1985.
[6] F. Baumgärtner, Chemie der Nuklearen Entsorgung, Teil II, Verlag Karl Thiemig, Munich, 1978.
[7] J.D. Navratil, J. Nucl. Sci. Technol. 26 (1989) 735.
[8] J.D. Navratil, W.W. Schulz, Journal of Mineral, Metal and Materials Society (JOM) 45 (1993) 32.
[9] Bundesrepublik Deutschland, Atomgesetz, Bundesgesetzblatt (BGBI) I (1998) 694.
[10] U. Wenzel, S. Deron, Solv. Extract. Ion Exchange 12 (1994) 789.
[11] U. Wenzel, W. Ullrich, M. Lochny, Nucl. Instr. Methods A 421 (1999) 567.
[12] E. Glueckauf, Trans. Faraday Soc. 51.1 (1955) 34.
[13] A. Hald, Statistical Tables and Formulas, Wiley, New York, 1952.
[14] J.J. van Deemter, F.J. Zuiderweg, A. Klingenberg, Chem. Eng. Sci. 5 (1956) 271.
[15] J.H. Knox, G.R. Laird, P.A. Raven, J. Chromatogr. 122 (1976) 129.

[16] T. Farkas, J.Q. Chambers, G. Guiochon, J. Chromatogr. A 679 (1994) 231.
[17] R.A. Shalliker, B.S. Broyles, G. Guiochon, J. Chromatogr. A 888 (2000) 1.
[18] R. Küpfner, H. Hofmann, Chem. Eng. Sci. 45 (1990) 2141.
[19] K. Schnitzlein, Chem. Eng. Sci. 48 (1993) 811.
[20] M. Lochny, Jül-3569 (1998) 58.